

## RESEARCH

### PREDICTION OF THE PROPERTIES OF POLYETHYLENE TEREPHTHALATE AND ITS CARBON NANOTUBE COMPOSITES

A. K. Gabitov, T. R. Prosochkina, K. G. Kichatov ✉

*Molecular dynamics modelling was carried out for polyethylene terephthalate and composite materials derived from this polymer with different single-walled carbon nanotubes as a filler. The effect of the supramolecular structure of this polymer composite material on some of its physicochemical and mechanical properties was studied. The interphase intermolecular interaction of the polymer matrix-filler system was found to be the major factor determining the physicochemical and mechanical properties. Therefore, consideration of this interaction is necessary for predicting the properties of such materials.*

**Keywords:** polyethylene terephthalate, carbon nanotube, molecular dynamics, intermolecular interactions, mechanical properties, elastic properties, Young's modulus.

An urgent need has arisen for new materials to advance industrial technology. Polymer composite materials (PCM) containing organic and inorganic fillers have attracted considerable interest because they possess a unique combination of properties. Significantly, the characteristics of PCM are a function not only of the properties of the polymer matrix but also of the nature of the filler, its shape and size, the properties of the phase separation surface, and the dispersion. The supramolecular structure of the polymer is altered upon the introduction of the filler, which leads to change in the physicochemical, mechanical, and working properties of the PCM [1].

Carbon nanotubes (CNT) and derived carbon materials have found use in the manufacture of PCM for strong ultralight parts with improved mechanical characteristics such as enhanced tensile strength as well as resistance to tearing and abrasion [2]. Thus, the Young's modulus of CNT is about 1 GPa [3], while the strength is about 30 GPa [4], which is much greater than the values of these parameters for steel, for which the corresponding value is only about 1 GPa.

Single-walled carbon nanotubes (SWCNT) are bands of graphene sheets (graphite monolayers) twisted into cylinders with tube diameter 5-20 Å [5]. Multi-walled carbon nanotubes (MWCNT) consist of several graphite sheets with tubular shape, which are arranged one on top of another with distance between two carbon layers in the side wall equal to 0.34 nm [6]. The Young's modulus, resistance to destruction under stress, and impact strength for SWCNT are 0.32-1.47 GPa, 10-52 GPa, and 770 J/g, respectively. The values of these parameters for MWCNT are 0.27-0.95 GPa, 11-63 GPa, and 1240 J/g, respectively. SWCNT

---

Ufa State Petroleum Technological University. Corresponding author: K. G. Kichatov ✉. E-mail: Kichatov\_k@mail.ru. Translated from *Khimiya i Tekhnologiya Topliv i Masel*, No. 1, pp. 43–49, January–February, 2024.

have good potential for improving the mechanical properties of composites due to a large specific molecular surface and lack of inactive internal layers. On the other hand, two-walled nanotubes, despite a smaller specific surface, do not readily agglomerate such that a smaller amount of the filler is needed in the production of PCM [7]. At present, the advantages and disadvantages of each type of nanotube can be evaluated only by studying the properties of specific derived PCM.

The electrical conductivity of CNT, which characterizes their electrical properties, is approximately one thousand times greater than for copper wire and the energy stability of CNT is higher than for fullerenes and graphene films [8].

However, the industrial production of PCM containing nanotubes is limited by the need to achieve homogeneous distribution of the nanotubes without undesirable agglomeration in the polymer matrix [9]. Agglomeration leads to low solubility and adhesion as well as to significant porosity and viscosity of PCM [10]. In addition, studies are underway on the functionalization of CNT to provide for chemical bonding of CNT with the base, for example, made of a plastic material, in order to optimize structural ordering in the resultant materials. Ultrasonic treatment or the addition of a deflocculant can be used for reducing the amount of CNT agglomeration by overcoming of the strong van der Waals interaction between the individual CNT molecules [11].

Polyethylene terephthalate (PET) is a well-known commercially produced polymer and has found use throughout the world in the chemical, food, and medical industries, as well as in machine building and the manufacture of household appliances. On the other hand, the use of this material is limited since its mechanical properties and thermal stability do not always meet the necessary requirements [12].

One way to improve the properties of PET is its modification by introducing various fillers [13]. For example, Chowreddy et al. [14] have shown that the introduction of 0.25 mass % multilayered CNT into PET leads to a significant increase in viscosity, crystallinity, crystallization temperature, thermal stability, glassy-point temperature, and ultimate tensile strength.

There are now three types of methods to produce CNT/polymer PCM: bulk polymerization, compounding in solution, and melt compounding. The latter method is the simplest and most efficient, especially for the industrial manufacture of the less expensive types of thermoplastics [15].

The preparation of PCM is a multistep process and the optimal procedure is often found by empirical testing [16]. An improved approach could involve modelling of the composite material using a modern programming package. The modelling of the structure of PCM would, as a rule, require the use of molecular mechanics (MM) [17], quantum chemistry [18], molecular dynamics (MD) [19], Monte Carlo (MC) [20], or finite element (FEM) methods [21]. Methods MM, MC, and MD allow us to model materials on the atomic level, which permits the design of new composites. The finite element method (FEM) is based on the approximation of a continuous medium, in which the object is considered as a continuum. Empirical constants are used to calculate the properties. In this case, modelling of materials from new substances whose parameters are not in the data base does not appear possible. Nevertheless, FEM is one of the major numerical methods used to calculate the parameters of composite materials. This method permits not only the design of new PCM but also prediction of the onset of delamination, cracks, and deformation [22].

The unique properties of CNT have sparked considerable interest in the experimental determination of the characteristics of PCM when they are added as fillers. The mechanical properties of such composite materials have been studied for polymer matrices, namely, polyethylene [23], polypropylene [24], polystyrene [25], polycarbonate [26], and epoxy resins [27]. Theoretical and computational methods have been concurrently developed for predicting the characteristics of PCM, including mechanical properties. Thus, Yazdani et al. [28] have studied the mechanical properties of low- and high-density polyethylene using MD methods. The effect of the polymer chain length, type and concentration of CNT, and deformation rate on the predicted mechanical properties was studied at different temperatures. Huang et al. [29] used FEM to calculate the viscoelastic properties of SWCNT/polypropylene nanocomposites depending on the temperature and SWCNT concentration. The effect of different SWCNT filler concentrations (0.1, 0.3, and 0.5 mass %) was analyzed experimentally and theoretically to evaluate the effect of the SWCNT parameters on the elasticity modulus of an SWCNT/epoxy resin PCM [30]. The elasticity modulus was found to increase with increasing SWCNT concentration up to 0.3% and then drop due to the formation of local agglomerates in the PCM. Modelling using the Digimat-FE program package showed the need to take account of the interphase interaction in the SWCNT-epoxy resin system as well as of the curvature and agglomeration of the SWCNT. The difference between the calculated and experimental data is reduced by taking account of the interphase interaction and agglomeration of the SWCNT. The relative discrepancy between

the experimental and calculated values of the elasticity modulus was 6.8% for the sample containing 0.1 mass % SWCNT. Furthermore, better results were obtained for this sample when modelling the SWCNT as curved elements taking account of agglomeration such that the relative error of the calculation was reduced to only 4.1%.

Liao and Li [31] used MM methods to show that the characteristics of polystyrene composite materials are largely a function of interphase intermolecular interactions of the CNT filler and the polystyrene matrix, while stress-strain arises due to discrepancies of the thermal expansion coefficients of the components of the composite.

Kumar et al. [19] used MD methods to study the effect of the volumetric fraction of the filler on the mechanic properties such as Young's modulus, shear modulus, and bulk modulus of nylon 6 reinforced with SWCNT. These results show that upon an increase in the SWCNT content from 2 to 4%, the longitudinal Young's modulus increases by 47.48%, while an increase in the SWCNT content from 4 to 8% leads to an increase in the longitudinal Young's modulus by 120%. These modelling results are in accord with the rule of mixtures.

Analysis of the effect of fillers such as CNT, carbon black, graphene, and clay on the characteristics of PET showed that CNT specifically can considerably improve the mechanical properties of the resultant material [15, 32-35]. Gómez-del Rio et al. [36] established that the Young's modulus for SWCNT-reinforced PET increases steadily with increasing bulk fraction of SWCNT along with a concurrent decrease in the Poisson coefficient, while the flow limit increases only slightly. On the other hand, the addition of SWCNT sharply reduces the fracture strain. Due to better dispersion of the carbon fillers in the PET matrix in comparison with other polymers, improvement of the mechanical, transport, electrical, and other operational properties can be achieved with lower filler content in comparison with traditional PCM, which would permit reducing the costs of their production [37]. However, along with the improved elastic modulus and strength, the addition of CNT filler to the PET matrix often leads to a reduction in flexibility thereby limiting the industrial uses of the PCM.

Bitenieks et al. [38] found that CNT/PET nanocomposites containing up to 5 mass % CNT form CNT bundles homogeneously distributed within the polymer matrix along with a bonded network structure, which significantly affects the properties of the material and increases its crystallinity. The addition of CNT leads to an increase in viscosity and modulus of elasticity. The rheological percolation threshold is 0.83 mass % CNT.

Alexiou et al. [13] came to the conclusion that the properties of reinforced PET are partially controlled by the morphology and molecular orientation of the polymer matrix. Readily dispersed MWCNT samples functionalized with 0.7% CO<sub>2</sub>H groups, length 10-20 mm, and external diameter 30-50 nm are used as fillers. The addition of such MWCNT to such systems leads to additional nucleation, increasing the crystallization of the PET matrix, lowering the anisotropy of the properties, and differentiating the orientation of the MWCNT relative to the macromolecular chains.

Analysis of the experimental studies showed that the change in the properties of the PCM with increasing filler fraction in the matrix, as a rule, proceeds nonlinearly. Hence, the systems cannot be described using standard models such as the rule of mixtures and the Maxwell model. On the other hand, this problem can be overcome by using percolation theory relating the sharp change in the system to formation of a percolation cluster consisting of nanoparticles. Shao et al. [39] also found that the Cox-Krenchel, Halpin-Tsai, and Mori-Tanaka micromechanical models are not suitable for accurate calculation of the mechanical characteristics of SWCNT/PET materials. The rule of mixtures is also not obeyed. However, the use of a hybrid method combining FEM and the Mori-Tanaka micromechanical model leads to good agreement of the calculated and experimental values of the Young's modulus by the introduction of an additional parameter for curvature of the SWCNT.

Ding et al. [40] noted that SWCNT are considered promising candidates as fillers for the mechanical reinforcement of polymers but their use is limited by their poor dispersion. In order to overcome this disadvantage, a film of SWCNT is deposited onto the PET surface by hot pressing. This procedure leads to a significant improvement in the mechanical and electrical properties as well as thermal stability of the PCM film even in the case of a very low mass fraction of SWCNT (0.066 mass %) due to the homogeneousness of the network structure of the SWCNT formed and a strong interphase interaction. The Young's modulus and tensile strength of the SWCNT/PET film reached 4.6 GPa and 148 MPa, respectively, which is 31.3% and 24.4% higher than for a film of pure PET.

Thus, the introduction of CNT into PET has been shown to improve the mechanical characteristics of PCM, leading to a worldwide increase in its use, primarily when a combination of high strength and light weight is required for manufactured items as in the case of pipes, structural elements, aviation and automobile parts, as well as in alternative energy installations. On the other hand, the potential of CNT for industrial use as fillers has not been fully realized. Thus, the production of PCM using CNT is considered a key technology for creating advanced next-generation composites [12]. However, there have been only a limited number of scientific publications devoted to the study of the effect of SWCNT on the properties of PCM, possibly due to the higher cost of this material in comparison to MWCNT and various technological problems. In contrast, computer modelling is a promising tool for studying the characteristics of such expensive PCM and finding the reasons causing the change in these properties. Hence, MD modelling has been carried out in an attempt to predict some mechanical properties of the SWCNT/PET system and we analyzed the effect of the geometrical parameters of SWCNT (diameter and length), which determine the dispersion properties, as well as the energy parameters of the interaction of the polymer matrix and filler, which, on the whole, govern the PCM properties.

A study of the mechanical properties of PET and SWCNT/PET was carried out using the MD method according to the procedures of Clark [41], Al Hasan [42], and Liu [43]. We used the Forcite and Amorphous Cell moduli to give the initial configuration of the PET and SWCNT atoms in order to form an amorphous PCM cell. Forcite, Forcite Geometry Optimization, and Forcite Dynamic modulus functions were used to find the equilibrium PCM geometry, while the Forcite Mechanical Properties program was used to calculate some mechanical properties.

Since carbon nanotubes can be seen as twisted graphene sheets, the chirality vector, which gives the direction of rotation, determines the geometrical configuration of a specific nanotube. The chirality vector is characterized by two chiral whole-number indices,  $n$  and  $m$ , which, in turn, give the chiral angle  $q$  and the CNT diameter [44].

Optimization of the geometrical parameters of PET and modelling of the cell structure for  $T = 298\text{K}$  using the COMPASS II force field was carried out for five types of material; polymer PET (**1**, **Fig. 1a**), SWCNT(4\_0)/PET PCM (**2**, **Fig. 1b**), SWCNT(4\_4)/PET (**3**, **Fig. 1c**), SWCNT(6\_0)/PET PCM (**4**, **Fig. 1d**), and SWCNT(6\_6)/PET PCM (**5**, **Fig. 1e**). The numbers and designations of the SWCNT correspond to the values of indices  $n$  and  $m$ , respectively.

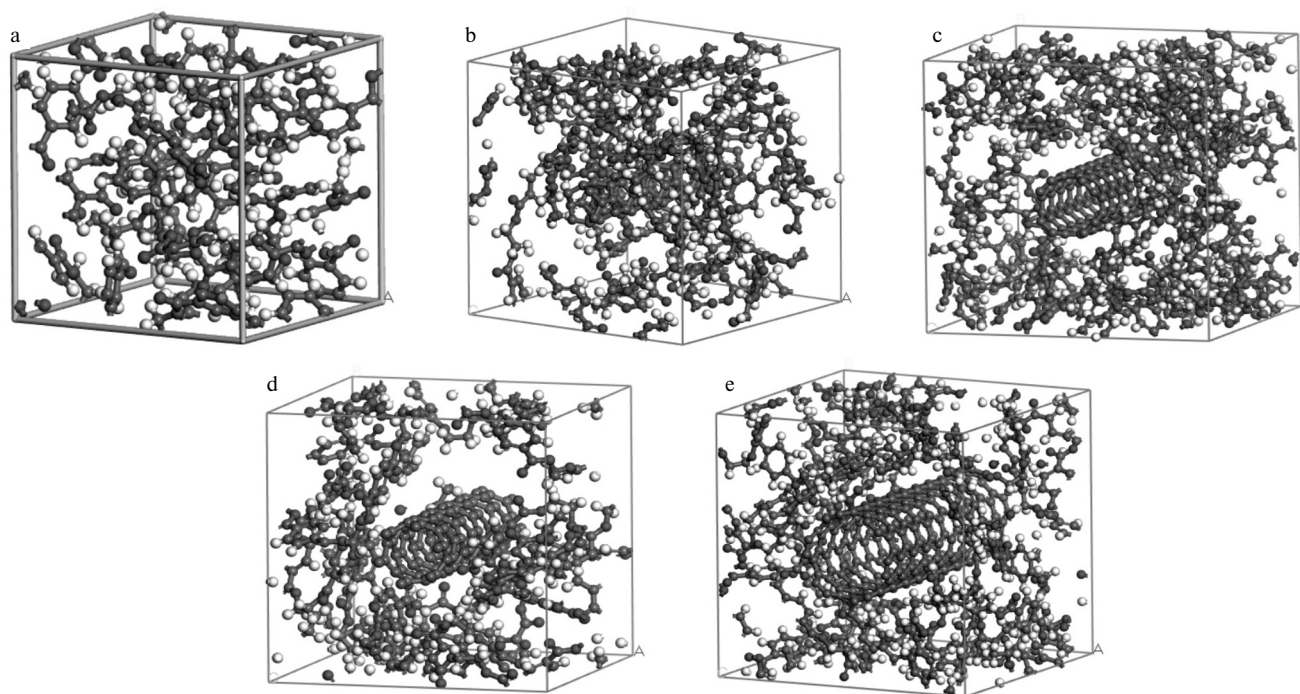


**Fig. 1. Periodic crystallographic cells used as calculation models**

Depending on the values of indices  $n$  and  $m$ , the SWCNT are classified as the achiral chair type for  $n = m$  (models SWCNT 4\_4 and SWCNT 6\_6) or the achiral zigzag type for  $m = 0$  (models SWCNT4\_0 and SWCNT6\_0) [45].

The NVT ensemble was selected to determine the pressure and density of the system under isochoric-isothermal conditions and the following parameters were used for the MD calculation: COMPASS II force field, Andersen thermostat,  $T = 298\text{K}$ , 1 fs time step, 50 ps total modelling time, fine precision. The pressure should be selected such that the calculated density of the material corresponds to the handbook value for PET ( $1.3\text{-}1.4\text{ g/cm}^3$ ) [46].

After selection of the pressure, the modelling was carried out assuming isobaric-isothermal conditions and the following PCM mechanical properties were determined: NPT ensemble, COMPASS II force field, Andersen thermostat,  $T = 298\text{K}$ , Berendsen barostat, time step 1.0 fs, total modelling time 50.0 ps, accuracy fine.

The constant strain rate method with eight steps for each strain and maximum stress amplitude 0.004 was used to calculate the elastic properties of PET.

Calculation of the mechanical properties of the SWCNT/PET PCM gave the Young's modulus characterizing the ability of the material to resist stretching and compression upon elastic deformation, Poisson coefficient giving the ratio of the relative transverse compression to relative longitudinal compression, shear modulus characterizing the ability of a material to resist shear strain, bulk modulus characterizing the ability of a material to resist all-around compression establishing the relationship between the relative change in the volume of a body and the pressure applied, and the Lamé coefficients characterizing elastic deformations of isotropic solid bodies belonging to the set of elasticity moduli. These calculations were carried out according to reported procedures [47-50].

The equilibrium geometrical characteristics of the nanotubes (**Table 1**) and energy parameters of the SWCNT/PET PCM (**2-5**) (**Table 2**) were obtained by optimization of the geometrical structure.

The energy contributions were calculated in accord with the formulas of Jaillet [52] and Gasteiger [53]:

$$E_{\text{total}} = E_{\text{bonded}} + E_{\text{non-bonded}}$$

$$E_{\text{bonded}} = E_{\text{val}} + E_{\text{cross}}$$

$$E_{\text{val}} = E_{\text{bond}} + E_{\text{angle}} + E_{\text{torsion}} + E_{\text{inversion}}$$

$$E_{\text{unbonded}} = E_{\text{electrostatic}} + E_{\text{Van der Waals}}$$

where  $E_{\text{total}}$  is the total energy of the system, kcal/mole;  $E_{\text{bonded}}$  is the intramolecular bond energy, kcal/mole;  $E_{\text{non-bonded}}$  is the intramolecular interaction energy, kcal/mole;  $E_{\text{val}}$  is the valence energy of the atoms, kcal/mole;  $E_{\text{cross}}$  is the energy of

**Table 1**

Parameter	Nanotube type			
	SWNT4_0	SWNT4_4	SWNT6_0	SWNT6_6
Diameter, Å	3.13	5.42	4.70	8.14
Length, Å	21.30	21.30	21.30	24.6

**Table 2**

Parameter, kcal/mole	Type of PCM			
	2	3	4	5
$E_{\text{total}}$	4278.4	7903.9	5914.1	10830.7
$E_{\text{val}}$	3664.6	7060.7	5273.9	10130.4
$E_{\text{bond}}$	105.2	200.5	100.3	182.2
$E_{\text{angle}}$	371.1	432.2	274.4	367.0
$E_{\text{torsion}}$	2948.6	6254.2	4729.4	9458.5
$E_{\text{inversion}}$	239.7	173.8	169.8	122.7
$E_{\text{cross}}$	-181.9	-354.6	-185.8	-345.8
$E_{\text{Van der Waals}}$	-283.0	-435.0	-274.0	-318.0
$E_{\text{electrostatic}}$	1099.5	1665.8	1121.3	1393.2
$E_{\text{non-bonded}}$	795.7	1197.8	826.0	1046.0

**Table 3**

Parameter	Type of PCM				
	1	2	3	4	5
Pressure, GPa	1.103	0.953	1.103	1.000	0.971
$E_x$ , GPa	2.6	7.8	15.6	11.3	5.1
$E_y$ , GPa	4.2	6.9	23.2	6.3	5.3
$E_z$ , GPa	3.0	24.7	56.1	22.9	32.9
$G_R$ , GPa	1.6	2.6	8.2	1.9	1.9
$G_V$ , GPa	2.2	3.6	9.9	3.2	3.7
$G_H$ , GPa	1.9	3.1	9.1	2.5	2.8
$B_R$ , GPa	7.0	13.1	17.6	11.4	9.2
$B_V$ , GPa	10.5	14.1	20.9	15.1	11.8
$B_H$ , GPa	8.7	13.6	19.2	13.3	10.5
$\lambda$ , GPa	7.8	16.7	23.5	19.8	17.2
$\mu$ , GPa	2.5	2.4	7.6	1.5	1.7
Compressibility, TPa <sup>-1</sup>	142.1	76.4	56.9	87.6	108.5
Density, g/cm <sup>3</sup>	1.4	1.5	1.4	1.4	1.4
$\nu_{12}$	0.29	0.3	0.4	0.2	0.2
$\nu_{21}$	0.39	0.4	0.4	0.2	0.04

cross-interactions (for example, simultaneous bond stretching and change in the bond angle), kcal/mole;  $E_{\text{bond}}$  is the bond stretching energy, kcal/mole;  $E_{\text{angle}}$  is the energy for change of bond angles, kcal/mole;  $E_{\text{torsion}}$  is the energy for change of torsion angles, kcal/mole;  $E_{\text{inversion}}$  is the electrostatic energy, kcal/mole;  $E_{\text{Van der Waals}}$  is the van der Waals energy, kcal/mole.

The calculated parameters for PET and SWCNT/PET are for the pressure calculated using the NVT ensemble and mechanical characteristics (Young's modulus along X, Y, Z axis ( $E_x$ ,  $E_y$ ,  $E_z$ ), shear modulus  $G$  and bulk modulus  $B$  averaged over Voigt, Reiss и Hill equations ( $G_V$ ,  $G_R$ ,  $G_H$ ,  $B_V$ ,  $B_R$ ,  $B_H$  respectively), Lamé coefficients ( $\lambda$ ,  $\mu$ ), compressibility, Poisson coefficients ( $\nu_{12}$ ,  $\nu_{21}$ ), and density) obtained upon modelling in the NVT ensemble given in **Table 3**.

The relationships of the values of elasticity moduli of PET without fillers and of CNT-reinforced PET given in Table 3 show much greater values of the Young's modulus and bulk modulus for the reinforced samples, suggesting improved mechanical properties for SWCNT/PET PCM relative to PET. **Table 4** gives the relative value of these elasticity parameters, which show how much greater these indices are for SWCNT/PET PCM in comparison with PET without filler. The greater values of Young's modulus are observed basically in the longitudinal direction (coefficient  $E_z$ ). This behavior is apparently related to the structure of the PCM, in which the modelling presupposes that the nanotube molecules line up along the Z-axis.

Best results for greater elasticity modulus relative to PET by itself are found for PCM **3** featuring single-walled nanotubes with diameter 5.42 Å and length 24.6 Å. The Young's modulus for this composite in the longitudinal direction is 18.5 times

**Table 4**

Parameter	Type of PCM			
	2	3	4	5
$E_x$ , GPa	3.0	6.0	4.3	1.9
$E_y$ , GPa	1.6	5.5	1.5	1.3
$E_z$ , GPa	8.1	18.5	7.6	10.8
$G_R$ , GPa	1.6	5.2	1.2	1.2
$G_V$ , GPa	1.6	4.4	1.4	1.6
$G_H$ , GPa	1.6	4.7	1.3	1.5
$B_R$ , GPa	1.9	2.5	1.6	1.3
$B_V$ , GPa	1.4	2.0	1.5	1.1
$B_H$ , GPa	1.6	2.2	1.5	1.2
Compressibility, TPa <sup>-1</sup>	1.86	2.50	1.62	1.31

greater than for pure PET. This finding most likely is related to higher intermolecular interaction energy (Table 2) than for the other PCM. On the other hand, the compressibility for PCM **3** is the lowest among the samples studied and 2.5 times lower than for PET without filler, indicating the greatest resistance of PCM **3** to bulk compression and, correspondingly, PCM **5** with diameter 8.14 Å and length 24.6 Å is characterized by lower resistance to bulk compression. The maximum discrepancy for the calculated density relative to the experimental value was found for PET without filler 0.28% ( $\Delta = 0.04 \text{ g/cm}^3$ ), while the calculated values for the Young's modulus in the X and Z directions were found to agree with the experimental results within the range of statistical error [54].

Regression analysis of the effect of various interaction energy contributions to the Young's modulus shows that a satisfactory level of correlation is found for increasing Young's modulus values with increasing van der Waals interactions:

$E_{\text{val}}$ .....	0.35
$E_{\text{bond}}$ .....	0.72
$E_{\text{angle}}$ .....	0.71
$E_{\text{torsion}}$ .....	0.32
$E_{\text{inversion}}$ .....	0.3
$E_{\text{cross}}$ .....	0.66
$E_{\text{Van der Waals}}$ .....	0.96
$E_{\text{electrostatic}}$ .....	0.84
$E_{\text{non-bonded}}$ .....	0.8

Thus, computer modelling of the amorphous cell containing CNT with different geometric parameters and of PET itself revealed that the geometrical arrangement of the nanotubes determines the intermolecular interaction in this system. The density of PET without filler obtained by modelling is close to the experimental result (0.28% discrepancy), which shows that our model is satisfactory. The calculations for the density of composite materials with low filler content can also be expected to have comparable satisfactory results.

In turn, the van der Waals interactions give rise to mechanical properties (Young's modulus, bulk modulus, and Poisson coefficient) with the  $R^2$  coefficient of determination 0.96, which would permit prediction of mechanical properties on the basis of the intermolecular interactions.

## REFERENCES

1. O. V. Kropotin et al., "Effect of carbon modifiers on the structure and wear resistance of polymer nanocomposites derived from polytetrafluoroethylene" [in Russian], *Zhurnal Tekhnicheskoi Fiziki*, **84**, No. 5, 66-70 (2014).
2. W. Khan, R. Sharma, and P. Saini, "Carbon nanotube-based polymer composites: Synthesis, Properties and Applications," *Carbon Nanotubes-Current Progress of their Polymer Composites*, Intech (2016).
3. M.-F. Yu, "Tensile loading of ropes of single wall carbon nanotubes and their mechanical properties," *Phys. Rev. Lett.*, **84**, No. 24, 5552-5555 (2000).
4. M.-F. Yu et al., "Strength and breaking mechanism of multiwalled carbon nanotubes under tensile load," *Science*, **287**, No. 5453, 637-640 (2000).
5. M. V. Kharlamova, "Advances in tailoring the electronic properties of single-walled carbon nanotubes," *Progr. Mater. Sci.*, **77**, 125-211 (2016).
6. E. Y. Pashkin et al., "The unexpected stability of multiwalled nanotubes under high pressure and shear deformation," *Appl. Phys. Lett.*, **109**, No. 8, 081904 (2016).
7. F. Gojny et al., "Influence of different carbon nanotubes on the mechanical properties of epoxy matrix composites," *Compos. Sci. Technol.*, **65**, Nos. 15-16, 2300-2313 (2005).
8. A. V. Eletsii, "Mechanical properties of carbon nanostructures and derived materials" [in Russian], *Uspekhi Fizicheskikh Nauk*, **177**, No. 3, 233-274 (2007).

9. N. T. Kakhramanov et al., "Nanostructured composites and polymer materials science" [in Russian], *Plasticheskie Massy*, Nos. 1-2, 49-57 (2016).
10. M. Choudhary et al., "Contemporary review on carbon nanotube (CNT) composites and their impact on multifarious applications," *Nanotechnol. Rev.*, **11**, No. 1, 2632-2660 (2022).
11. N. M. Nurazzi et al., "Mechanical performance and applications of CNTs reinforced polymer composites-a review," *Nanomaterials*, **11**, No. 9, 2186 (2021).
12. J. Young, S. Hun, *Nanocomposites-New Trends and Developments*, New Trends and Developments, InTech (2012).
13. V. F. Alexiou et al., "Poly(ethylene terephthalate) carbon-based nanocomposites: a crystallization and molecular orientation study," *Polymers (Basel)*, **12**, No. 11, 2626 (2020).
14. R. R. Chowreddy, K. Nord-Varhaug, F. Rapp, "Recycled polyethylene terephthalate/carbon nanotube composites with improved processability and performance," *J. Mater. Sci.*, **53**, No. 9, 7017-7029 (2018).
15. O. Rodriguez-Uicab et al., "Influence of processing method on the mechanical and electrical properties of MWCNT/PET composites," *J. Mater.*, **2013**, 1-10 (2013).
16. Q. H. Zeng, A. B. Yu, G. Z. Lu, "Multiscale modeling and simulation of polymer nanocomposites," *Prog. Polym. Sci.*, **33**, No. 2, 191-269 (2008).
17. J. Zhou et al., "Molecular mechanics-based design of high-modulus epoxy to enhance composite compressive properties," *Compos. Sci. Technol.*, **229**, 109678 (2022).
18. G. Alzubi Feras, R. Cosby, "Young's Modulus of Short Single-Wall Carbon Nanotubes: An Atomistic Simulation," *Advanced Materials: TechConnect Briefs*, 137-140 (2015).
19. U. Kumar et al., "Molecular dynamics simulation of Nylon/CNT composites," *Mater. Today Proc.*, **5**, No. 14, 27710-27717 (2018).
20. K. Zhao et al., "Monte Carlo simulation for exploring the mechanical properties of particle-reinforced composites based on the scale boundary finite element method," *Compos. Struct.*, **297**, 115933 (2022).
21. N. Gariya, B. Prasad, and P. Kumar, "FEM based analysis of soft polymer composites with crack," *Mater. Today Proc.*, **28**, 2426-2430 (2020).
22. Gopalraj S. Karuppanan, T. Kärki, "A finite element study to investigate the mechanical behavior of unidirectional recycled carbon fibre/glass fibre-reinforced epoxy composites," *Polymers (Basel)*, **13**, No. 18, 3192 (2021).
23. A. M. Najipour, A. Fattahi, "An experimental study on mechanical properties of PE/CNT composites," *Journal of Theoretical and Applied Mechanics*, 719 (2017).
24. Y. Liu et al., "Structure and tensile properties of polypropylene/carbon nanotubes composites prepared by melt extrusion," *Materials Science-Poland*, **32**, No. 3, 442-447 (2014).
25. O. A. Moskalyuk et al., "Mechanical performance of polystyrene-based nanocomposites filled with carbon allotropes," *Applied Sciences*, **13**, No. 6, 4022 (2023).
26. P. Raj, R. Kumar, *A Brief Review: Study on Mechanical Properties of Polycarbonate with Different Nanofiller Materials*, (2021), pp. 285-291.
27. A. S. Krieg et al., "Mechanical properties and characterization of epoxy composites containing highly entangled as-received and acid treated carbon nanotubes," *Nanomaterials*, **11**, No. 9, 2445 (2021).
28. H. Yazdani et al., "Mechanical properties of carbon nanotube-filled polyethylene composites: a molecular dynamics simulation study," *Polym. Compos.*, **40**, No. S2 (2019).
29. J. Huang, D. Rodrigue, L. Dong, "Effect of temperature on the viscoelastic properties of carbon nanotube reinforced polypropylene composites," *Advances in Materials Science and Engineering*, **2021**, 1-12 (2021).
30. M. A. Maghsoudlou et al., "Effect of interphase, curvature and agglomeration of SWCNTs on mechanical properties of polymer-based nanocomposites: experimental and numerical investigations," *Compos. B Eng.*, **175**, 107119 (2019).
31. K. Liao, S. Li, "Interfacial characteristics of a carbon nanotube-polystyrene composite system," *Appl. Phys. Lett.*, **79**, No. 25, 4225-4227 (2001).



32. L. Qiao et al., "Mechanical properties, melting and crystallization behaviors and morphology of carbon nanotubes/continuous carbon fiber reinforced polyethylene terephthalate composites," *Polymers*, **14**, No. 14, 2892 (2022).
33. S. Yesil, G. Bayram, "Effect of carbon nanotube surface treatment on the morphology, electrical, and mechanical properties of the microfiber-reinforced polyethylene/poly(ethylene terephthalate)/carbon nanotube composites," *J. Appl. Polym. Sci.*, **127**, No. 2, 982-991 (2013).
34. J. Y. Kim, H. S. Park, S. H. Kim, "Multiwall-carbon-nanotube-reinforced poly(ethylene terephthalate) nanocomposites by melt compounding," *J. Appl. Polym. Sci.*, **103**, No. 3, 1450-1457 (2007).
35. B. A. Alshammari, A. Wilkinson, "Impact of carbon nanotubes addition on electrical, thermal, morphological, and tensile properties of poly(ethylene terephthalate)," *Appl. Petrochem. Res.*, **6**, No. 3, 257-267 (2016).
36. T. Gómez-del Rio et al., "Influence of single-walled carbon nanotubes on the effective elastic constants of poly(ethylene terephthalate)," *Compos. Sci. Technol.*, **70**, No. 2, 284-290 (2010).
37. A. K. Singh, R. Bedi, B. S. Kaith, "Composite materials based on recycled polyethylene terephthalate and their properties-a comprehensive review," *Compos. B Eng.*, **219**, 108928 (2021).
38. J. Bitenieks et al., "Dynamic mechanical, dielectrical, and rheological analysis of polyethylene terephthalate/carbon nanotube nanocomposites prepared by melt processing," *Int. J. Polym. Sci.*, **2020**, 1-7 (2020).
39. L. H. Shao et al., "Prediction of effective moduli of carbon nanotube-reinforced composites with waviness and debonding," *Compos. Struct.*, **87**, No. 3, 274-281 (2009).
40. W.-T. Ding et al., "Enhancing the electrical conductivity and strength of PET by single-wall carbon nanotube film coating," *ACS Appl. Mater. Interfaces*, **15**, No. 31, 37802-37809 (2023).
41. S. J. Clark et al., "First principles methods using CASTEP," *Z. Kristallogr. Cryst. Mater.*, **220**, Nos. 5-6, 567-570 (2005).
42. N. H. J. Al Hasan, "Prediction of mechanical properties of EPON 862 (DGEBA) cross-linked with curing agent (TETA) and SiO<sub>2</sub> nanoparticle based on materials studio," *IOP Conf. Ser. Mater. Sci. Eng.*, **454**, 012139 (2018).
43. B. Liu et al., "Molecular dynamics study of the influence of nano SiO<sub>2</sub> on the thermodynamic properties of PMIA Composites," *Polymers*, **14**, No. 15, 3134 (2022).
44. M. L. D. Aydin, "Vibroelectronic properties of functionalized single-walled carbon nanotubes and double-walled boron nitride nanotubes," *Physical and Chemical Properties of Carbon Nanotubes*, InTech (2013).
45. T. Michel et al., "About the indexing of the structure of single-walled carbon nanotubes from resonant Raman scattering," *Advances in Natural Sciences: Nanoscience and Nanotechnology*, **1**, No. 4, 045007 (2010).
46. A. K. van der Vegt, L. E. Govaert, *Polymeren: van Ketten tot Kunststof*, DUP Blue Print (2003).
47. Y. Mo, H. Zheng, J. Xu, "Molecular dynamic simulation of the mechanical properties of PI/SiO<sub>2</sub> nanocomposite based on materials studio," *J. Chem. Pharm. Res.*, **6**, 1534-1539 (2014).
48. B. Yang et al., "Molecular dynamics study on the reinforcing effect of incorporation of graphene/carbon nanotubes on the mechanical properties of swelling rubber," *Polym. Test.*, **102**, 107337 (2021).
49. R. Anjana, S. Sharma, and A. Bansal, "Molecular dynamics simulation of carbon nanotube reinforced polyethylene composites," *J. Compos. Mater.*, 002199831667426 (2016).
50. N. B. Shenogina et al., "Molecular modeling approach to prediction of thermos-mechanical behavior of thermoset polymer networks," *Macromolecules*, **45**, No. 12, 5307-5315 (2012).
51. A. S. Kravchuk and A. I. Kravchuk, "Method for averaging the elastic properties of a composite from components with considerably different elasticity parameters" [in Russian], *Perspektivy Nauki*, **10**, No. 121, 27-32 (2019).
52. I. Jaillet, S. Artemova, and S. Redon, "IM-UFF: Extending the universal force field for interactive molecular modeling," *J. Mol. Graph Model.*, **77**, 350-362 (2017).
53. J. Gasteiger, T. Engel, *Chemoinformatics: A Textbook*, Wiley-VCH (2003), pp. 338-349.
54. D. A. Beeva et al., "Thermoplastic Composition Based on Polysulfone," *US Patent 2,477,735* (2013).